MYCOLOGY
2025, VOL. 16, NO. 2, 903–917
https://doi.org/10.1080/21501203.2024.2408259

Taylor & Francis
Taylor & Francis Group

RESEARCH ARTICLE

OPEN ACCESS Check for updates

Transcriptome analysis of Ochratoxin a (OTA) producing *Aspergillus westerdijkiae* fc-1 under varying osmotic pressure

Yanling Ma[a*], Muyuan Zhuang[a*], Tanvir Ahmad[a], Mingxuan Li[a,b], Guangyou Tan[a], Yingyao Deng[a] and Yang Liu[a]

[a]School of Food Science and Engineering, Foshan University/National Technical Center (Foshan) for Quality Control of Famous and Special Agricultural Products/Guangdong Key Laboratory of Food Intelligent Manufacturing, Foshan, China; [b]Guangdong Provincial Key Laboratory of Protein Function and Regulation in Agricultural Organisms, College of Life Sciences, South China Agricultural University, Guangzhou, China

ABSTRACT

Ochratoxin A (OTA) is a toxic secondary metabolite produced by the *Aspergillus* species which can contaminate various food products. This study analysed the transcriptome of the *Aspergillus westerdijkiae* fc-1 strain under NaCl concentrations of 0, 20, and 100 g/L using RNA-Seq technology to examine gene transcriptional changes linked to osmotic stress and OTA production. Significant changes were observed in metabolic-pathways associated with carbohydrates, cellular communication, and hydrolase activity under 20 g/L NaCl. The *HOG1* gene, associated with osmotic pressure regulation was down-regulated by 78.06%. In contrast, OTA biosynthesis genes *otaA*, *otaB*, and *otaC* were up-regulated by 3.26 fold, 1.99 fold, and 2.06 fold, respectively. Conversely, the *otaD* gene was down-regulated by 43.50%. At 100 g/L NaCl, pathways related to ion transport, peptide metabolism, ribosomal function, and transmembrane transporter protein activities were significantly up-regulated. The *HOG1* gene was up-regulated by 28.32% and OTA biosynthesis genes *otaA*, *otaB*, *otaC*, and *otaD* showed up-regulation of 27.06%, 36.80%, 19.59%, and 5.72 fold, respectively. The study highlights the role of metabolic pathways in osmotic stress regulation and the correlations between *HOG1* expression and OTA biosynthesis genes, providing insights for developing strategies to prevent OTA contamination in food.

ARTICLE HISTORY
Received 18 July 2024
Accepted 19 September 2024

KEYWORDS
OTA; *Aspergillus westerdijkiae*; NaCl; RNA-Seq; *HOG* signalling cascade

1. Introduction

Aspergillus species are the most common fungi that produce OTA, a toxin commonly found in various types of foods and feed products, posing a significant and serious health threat to humans and animals (Hesseltine et al. 1972; Cabañes et al. 2010; Navale et al. 2021). The International Agency for Research on Cancer (IARC) has classified OTA as a Group 2B potential human carcinogen. OTA causes immunotoxicity, neurotoxicity, and genotoxicity (Anli and Alkis 2010; Pyo et al. 2021). *Aspergillus westerdijkiae* is known to be one of the most significant producers of OTA. It commonly contaminates food products, including beverages, grapes, wheat, coffee beans, and dry pickles. Therefore, it is essential to prevent and control OTA-producing strains in foods (Cabañas et al. 2008; Vipotnik et al. 2017; Altafini et al. 2019; Chen et al. 2022; Wei et al. 2022).

The researchers have found various types of genes, including the polyketide synthase (PKS) encoding gene *otaA*, the non-ribosomal peptide synthase (NRPS) encoding gene *otaB*, the P450 oxidase encoding gene *otaC*, and the halogens encoding gene *otaD* are associated with OTA biosynthesis (Hussein et al. 2024). In the OTA biosynthesis process, the PKS and *otaD* genes are responsible for initiating and completing the OTA synthesis, respectively (Geisen et al. 2004; Gallo et al. 2013; Ferrara et al. 2016). New genes related to OTA production known as *AoOTApks* were discovered and found to be positively correlated (Wang et al. 2015). A notable correlation was found between the expression profile of *AcOTApks* and OTA production kinetics (Gallo et al. 2014). The OTA biosynthesis-pathway remains incompletely understood even though lots of studies have been conducted in various OTA-producing fungal isolates and specific genes have been identified. These genes include PKS, needed for biosynthesis of dihydro-coumarin precursors, and non-ribosomal-peptide synthetase (NRPS) (O'Callaghan et al. 2013; Gerin et al. 2016).

CONTACT Yang Liu liuyang@fosu.edu.cn; Tanvir Ahmad tanvir@fosu.edu.cn School of Food Science and Engineering, Foshan University, 33 Guangyun Road, Shishan Town, Nanhai District, Foshan 528231, China

*Yanling Ma and Muyuan Zhuang have contributed equally to this work.

© 2024 The Author(s). Published by Informa UK Limited, trading as Taylor & Francis Group.
This is an Open Access article distributed under the terms of the Creative Commons Attribution-NonCommercial License (http://creativecommons.org/licenses/by-nc/4.0/), which permits unrestricted non-commercial use, distribution, and reproduction in any medium, provided the original work is properly cited. The terms on which this article has been published allow the posting of the Accepted Manuscript in a repository by the author(s) or with their consent.

Recent findings have shown that OTA is produced through a series of steps. First, 7-methylmalonic is synthesised by PKS using acetyl-coenzyme A and malonyl-coenzyme A. Then, 7-methylmalonic acid is oxidised to OTB by cytochrome monooxygenase (*otaC*). OTB then reacts with L-β-phenylalanine to produce OTB through an amide bond, facilitated by the NRPS-*otaB* enzyme. Finally, OTB is chlorinated to produce OTA by the halogenase enzyme (*otaD*) (O'Callaghan et al. 2003; Wang et al. 2018).

However, the production of fungal mycelium growth and OTA biosynthesis are primarily influenced by environmental factors. Osmolarity is considered one of the most important environmental factors, and OTA contamination is also widespread in dry cured foods with high NaCl content (Wang et al. 2023). It seems that OTA biosynthesis is associated with NaCl rich substrates. Osmotic pressure changes induced by NaCl are often transmitted to the transcriptional level through the high osmolarity glycerol mitogen-activated-protein-kinase (*HOG*-MAPK) signalling pathway, which is the primary pathway involved in responding to osmotic stress (Schmidt-Heydt et al. 2011; Stoll et al. 2013). For *Penicillium nordicum* and *Penicillium verrucosum* strains, the biosynthesis of OTA was correlated with the phosphorylation of *HOG* MAP kinase induced by NaCl (Stoll et al. 2013; Wang et al. 2016). The *AwHOG1* gene deletion significantly impacted *A. westerdijkiae* colony morphology, mycelial growth, sporulation, OTA accumulation, and infective capacity. It also increased the mutant's sensitivity to high osmotic pressure (Wang et al. 2023). The osmotic pressure environmental factor responded to the activation of the *HOG* pathway, and different NaCl conditions had a significant effect on OTA production (Schmidt-Heydt et al. 2012). Furthermore, other metabolic pathways, such as carbon metabolism, ribosomes, cellular communication, and peptide metabolic processes are closely related to the production of fungus mycelium growth and biosynthesis of mycotoxins (Corrochano et al. 2016; Wei et al. 2022).

RNA sequencing (RNA-seq) is extensively used to study osmotic pressure regulatory pathways. It is an effective tool for analysing transcriptomes and has been magnificently employed to analyse differential gene expression in fungal metabolic pathways and transcriptomes under different NaCl conditions (Novodvorska et al. 2013). In this study, RNA-Seq technology was used to understand the role of genes involved in OTA synthesis, secondary metabolic processes, *HOG* pathway, and other metabolic pathways in the *A. westerdijkiae* fc-1 strain under different NaCl concentrations. The exposure of this regulatory mechanism can help to develop effective control strategies to reduce food contamination by OTA. The study conducted transcriptome analysis to examine how different levels of NaCl affect gene expression and metabolic pathways, particularly the *HOG* pathway in the *A. westerdijkiae* fc-1 strain. By analysing changes in the expression of *HOG1* and *otaA–D* biosynthesis genes along with qRT-PCR results, this study aimed to understand the factors influencing the growth and OTA production in *A. westerdijkiae* fc-1. The findings will be valuable for developing effective strategies to minimise OTA contamination in food.

2. Materials and methods

2.1. Fungal strain and culture medium

In this study, *A. westerdijkiae* fc-1 (Wei et al. 2022) was activated and cultured on potato dextrose agar medium (PDA) and incubated at 28 °C for 7 d. The spores were scraped from a PDA plate with a sterilised cotton swab and then resuspended in sterile distilled water. The pore suspension (10^7 spores/mL) was kept at −80 °C with 15% glycerol solution (Wang et al. 2020).

2.2. Extraction of RNA, construction of libraries, and sequencing using Illumina technology

A 100 µL of spore suspension was inoculated into PDA culture medium and incubated at 28 °C for 3 d. Subsequently, 100 mL PDB solutions with NaCl concentrations of 0, 20, and 100 g/L were prepared and transferred into 250 mL conical flasks in triplicate. After sterilisation, the NaCl-containing PDB was inoculated with fungal mycelium and incubated at 160 r/min at 28 °C for 3 d. The mycelium was collected and transferred into 100 mL centrifuge tubes, then centrifuged at 10,000 r/min for 5 min. The supernatant was filtered and spores were collected for total RNA extraction under 0, 20, and 100 g/L NaCl conditions with three replications for each condition resulting in a total of 9 samples for sequencing analysis (Table 2). Poly(A) mRNA was enriched using oligo(dT) magnetic beads, fragmented with divalent cations in

the NEB Fragmentation Buffer, and the library was constructed following the NEB standard protocol (Parkhomchuk et al. 2009). The first strand of cDNA was generated using fragmented mRNA as a template and random oligonucleotides as primers in the M-MuLV reverse transcriptase system. Afterwards, the RNA strand was degraded with RNaseH, and the second strand of cDNA was synthesised with dNTPs in the DNA polymerase I system. The purified double-stranded cDNA underwent end-repair and A-tailing attachment of sequencing adapters. cDNA fragments around 250–300 bp were selected using AMPure XP beads, followed by PCR amplification. The PCR products were purified again with AMPure XP beads, resulting in the final libraries. The NEBNext® Ultra™ RNA Library Prep Kit for Illumina® was used for library construction. Afterwards, the Qubit 2.0 Fluorometer provided a preliminary quantification, and the library was diluted to 1.5 ng/μL. The insert size was then assessed using an Agilent 2100 bioanalyzer. Once the insert size met expectations, qRT-PCR was employed to accurately quantify the library's effective concentration, ensuring it exceeded 2 nmol/L for quality assurance.

2.3. Gene ontology (GO) function annotation of differently expressed genes (DEGs) and kyoto encyclopedia of genes and genomes (KEGG) pathway differential gene analysis

Cluster-Profiler software (Lamarre et al. 2008) was used for GO and KEGG enrichment analysis on the differential gene sets. Enrichment analysis was carried out using the hyper-geometric distribution principle. It involved using a set of differential genes obtained from the significant differential analysis and annotated to the GO or KEGG database as the differential gene set. The background gene set comprised of all genes subjected to significant differential analysis and annotated to the GO or KEGG database. For GO functional enrichment, a padj value of less than 0.05 was set as the threshold for significance. The top 30 most significant terms from the GO enrichment analysis were selected for histogram visualisation, or all available terms were used if fewer than 30 were identified. These histograms were organised into categories of biological processes, cellular components, and molecular functions and also illustrated the up-regulation and down-regulation of differential genes. KEGG pathway enrichment analysis was performed using Cluster-Profiler software, with a padj value of less than 0.05 as the threshold for significance. This analysis focused on differentially expressed genes in the *A. westerdijkiae* fc-1 strain under three NaCl concentrations (0, 20, 100 g/L). Similarly, the top 30 most significant terms from the GO enrichment analysis were selected for histogram visualisation; if fewer than 30 terms were available, all terms were included. The results were summarised by major categories such as biological processes, cellular components, and molecular functions, and histograms were created to illustrate both up-regulation and down-regulation of differential genes.

2.4. Gene expression studies

Aspergillus westerdijkiae fc-1 strain cultured in a PDB medium with 0, 20, and 100 g/L concentrations of NaCl at 28 °C, and gene expression levels of *otaA*, *otaB*, *otaC*, *otaD*, and *HOG1* related to OTA synthesis were detected on the 3 d of post inoculation (dpi). Primers designed for target gene detection are shown in Table 1. The RNA concentration of the strain under 0, 20, and 100 g/L NaCl conditions was measured to be 56.8, 120.1, and 397.4 ng/μL, respectively, by using an ultra-micro UV spectrophotometer (Quawell Q3000). cDNA was synthesised from RNA using M-MLV reverse transcriptase. Gene expressions under specific conditions were evaluated using qRT-PCR. Relative gene expression levels were calculated with CFX Manager software (Bio-Rad Laboratories) using the $2^{-\Delta\Delta CT}$ method and third parallel replicates (Bai et al. 2017).

Table 1. Primers were used to amplify *otaA*, *otaB*, *otaC*, *otaD*, and *HOG1* through qRT-PCR.

Primer name	Sequence (5′ to 3′)
otaA-F	TCGAGCGCATGATACACGTT
otaA-R	ATGCGTTTGATGCGCCATTT
otaB-F	CAAGCATGGCGACAATAGCC
otaB-R	ACCCGGATCATATTGCCGTC
otaC-F	GAGGTGATAATGTCGGCGGT
otaC-R	GTGCTCTGATCGCTCCCTAC
otaD-F	ACTCCGCGATTCTATGCCAG
otaD-R	CTTGGTTGCCATCTCCTGGT
HOG1-F	CCACCTCCACGTCGTACTT
HOG1-R	ACCTCAAACCCAGCAACATC
18s-F	ATGGCCGTTCTTAGTTGGTG
18s-R	GAGCCGATAGTCCCCCTAAG

3. Results

3.1. Analysis of RNA sequencing and differential gene expression

The raw sequencing data included some reads with adapters and low-quality sequences. To ensure data reliability, these reads were filtered out, removing adapter-containing reads, reads with undetermined bases (N), and low-quality reads (where Qphred ≤ 20 bases constituted more than 50% of the read length). After filtering, sequencing errors and GC content distribution were checked, resulting in high-quality clean reads for further analysis. As shown in Table 2, the Q30 standard was met by over 91% of the bases, with GC content ranging from 35% to 65%. After de novo assembly, 389,403,562 genes were obtained, with an average length of 643.2 bp, indicating high sequencing quality suitable for further analysis.

Co-expression Venn diagrams display the genes uniquely expressed in each treatment group and indicate the number of genes co-expressed in two or more groups (Figure 1). A total of 11,391 differentially expressed genes (DEG; FC > |2|, FDR 0.05) were identified and functionally analysed by comparing the conditions of 0 g/L, 20 g/L, and 100 g/L NaCl. The lowest number of genes was found in the 0 g/L NaCl condition (Set1), the second highest in the 100 g/L NaCl condition (Set3), and the highest in the 20 g/L NaCl condition (Set2). A total of 9,210 genes were compared among the 0 g/L, 20 g/L, and 100 g/L NaCl conditions (Set7). The highest number of differentiated genes was 579 in the 0 g/L NaCl condition compared with the 20 g/L NaCl condition (Set4), the second highest number was 292 in the 20 g/L NaCl condition compared with the 100 g/L NaCl condition (Set6), and the highest number was 579 in the 0 g/L NaCl condition compared with the 100 g/L NaCl condition (Set6). The comparison of

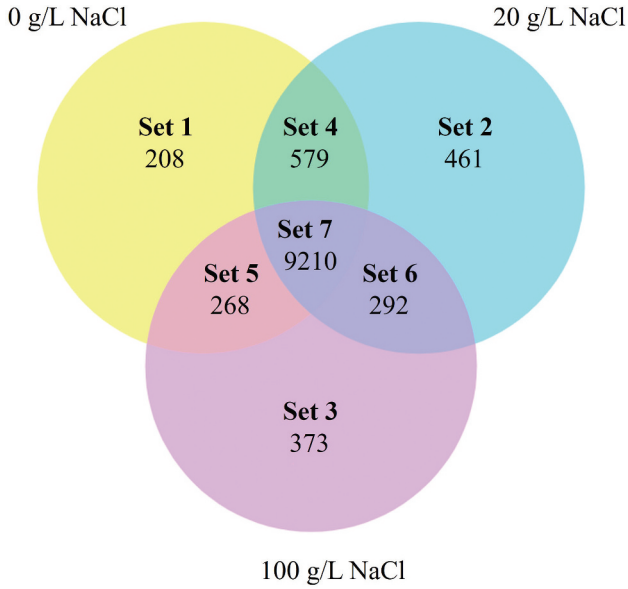

Figure 1. Wayne plots of DEG (FC > |2|), comparing differential genes under 0, 20, or 100 g/L NaCl condition.

the 0 g/L NaCl condition with the 100 g/L NaCl condition had the lowest number of differential genes at 268 (Set5). The volcano plot can visualise the distribution of differential genes in each comparison combination, as shown in Figure 2. In the experimental group with a salt concentration of 20 g/L NaCl, there were 13,228 DEGs compared to the control group with 0 g/L NaCl. Among these, 740 DEGs were up-regulated, and 575 DEGs were down-regulated (Figure 2A). In the experimental group with a salt concentration of 100 g/L NaCl, there were 12,941 DEGs compared to the control group (0 g/L NaCl). Within this group, 560 DEGs were up-regulated and 736 DEGs were down-regulated (Figure 2B). When comparing the experimental group with a salt concentration of 100 g/L NaCl to the control group with 20 g/L NaCl, there were a total of 13,040 DEGs. Among these, 1,015 DEGs were up-regulated and 1,324 DEGs were down-regulated (Figure 2C).

Table 2. Transcriptome sequencing summary of clean reads, error rate, Q30, and GC content for *Aspergillus westerdijkiae* fc-1 strain under different NaCl conditions.

Sample	Clean reads	Error rate (%)	Q30 (%)*	GC content (%)**
0 g/L NaCl_1	40,432,082	0.03	92.17	52.02
0 g/L NaCl_2	45,308,350	0.03	92.25	52.93
0 g/L NaCl_3	45,158,254	0.03	92.53	53.73
20 g/L NaCl_1	41,206,246	0.03	91.93	50.62
20 g/L NaCl_2	43,917,242	0.03	92.26	48.36
20 g/L NaCl_3	39,787,190	0.03	91.99	48.94
100 g/L NaCl_1	42,458,998	0.03	92.49	51.24
100 g/L NaCl_2	45,524,248	0.03	92.22	50.87
100 g/L NaCl_3	45,610,952	0.03	92.12	53.29

*Q > 30% is the percentage of bases with a mass value greater than 30 in the total bases with an error rate < 0.1%;
**GC (%) is the percentage of G and C bases in the total bases in the filtered reads count.

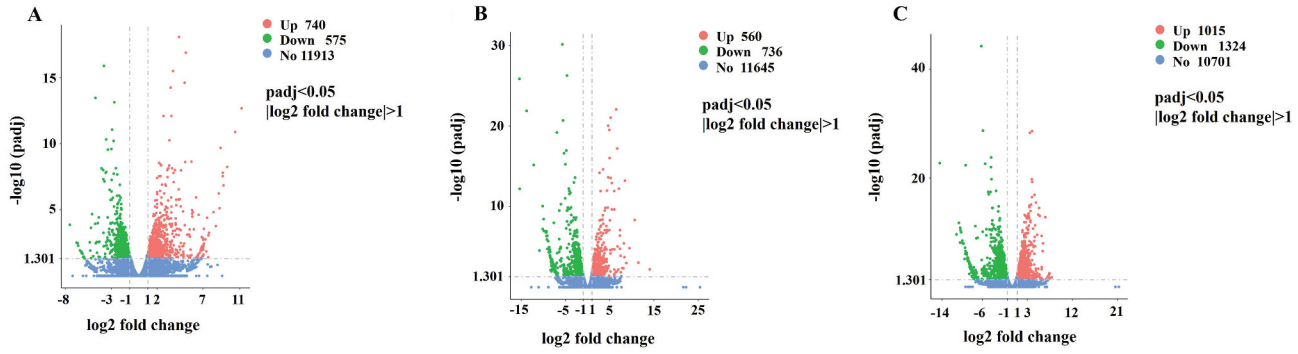

Figure 2. Volcano plots of differential gene expression under different osmotic pressure conditions. (A) 20 g/L NaCl vs. 0 g/L NaCl. (B) 100 g/L NaCl vs. 0 g/L NaCl. (C) 100 g/L NaCl vs. 20 g/L NaCl. The horizontal axis represents gene fold-changes (log2 fold change), and the vertical axis shows the significance of gene expression differences (−log10 padj). Red dots represent up-regulated genes, and green dots represent down-regulated genes.

3.2. Differential gene function analysis

GO (Gene Ontology) is a comprehensive database that describes gene function, cellular components, and molecular function. At a NaCl concentration of 20 g/L compared to a NaCl concentration of 0 g/L, the most significant numbers of genes enriched in biological processes were in carbohydrate metabolic processes, cellular communication, and signalling. There were no differentially expressed genes and no significant changes in cellular composition. The most significant gene enrichment in molecular function was in hydrolase activity and isomerase activity (Figure 3A). While a NaCl concentration of 100 g/L compared to a NaCl concentration of 0 g/L, the genes of high to low significance in biological processes were ion transport and ion transmembrane transport. In cellular composition, significance was high in cytoplasm, ribosomes, ribosomal protein complexes, and mitochondria. In molecular function, the significance in descending order is ribosomal protein complex, structural molecular activity, transport activity, and transmembrane transporter protein activity (Figure 3B). The significance of a NaCl concentration of 100 g/L compared to a NaCl concentration of 20 g/L was observed in various biological processes. In descending order, the significance was observed in the organic nitrogen compound biosynthesis process, translation, peptide metabolism process, peptide biosynthesis process, and cytosolic amide metabolism process. In terms of cellular composition, the significance from higher to lower was associated with ribosomes, cytoplasm, and protein complexes. In molecular function, higher significance was seen in structural molecular activity and ribosomal structural components (Figure 3C).

3.3. Differential gene KEGG function analysis

From the KEGG enrichment results, the 20 most significant KEGG pathways were selected to be plotted in a scatter plot for presentation. If there were fewer than 20, all the pathways were plotted, as shown in Figure 4. When comparing a NaCl concentration of 20 g/L to 0 g/L, the number of differentially enriched genes within KEGG-enriched pathways was identified. These pathways were listed in descending order of the number of genes they contain, including the Carbon Metabolism pathway, the Glycolysis pathway, the Glyoxylate and Dicarboxylic Acid Metabolism pathway, the Galactose Metabolism pathway, the MAPK Signaling pathway. Furthermore, in descending order of their significance, the pathways observed were Glycolysis, Carbon Metabolism, Fructose and Mannose Metabolism, the Pentose Phosphate pathway, and the MAPK Signaling pathway (Figure 4A). When the NaCl concentration was 100 g/L compared to 0 g/L, the ribosomal pathway, oxidative phosphorylation pathway, and carbon metabolism pathway showed the highest enrichment of differential genes in KEGG-enriched pathways (Figure 4B). When the concentration of NaCl was 100 g/L compared with NaCl 20 g/L, the KEGG-enriched pathways in which the number of differentially enriched genes was higher and significant were the ribosomal pathway, carbon metabolism pathway, oxidative phosphorylation pathway, pyruvate metabolism pathway, and

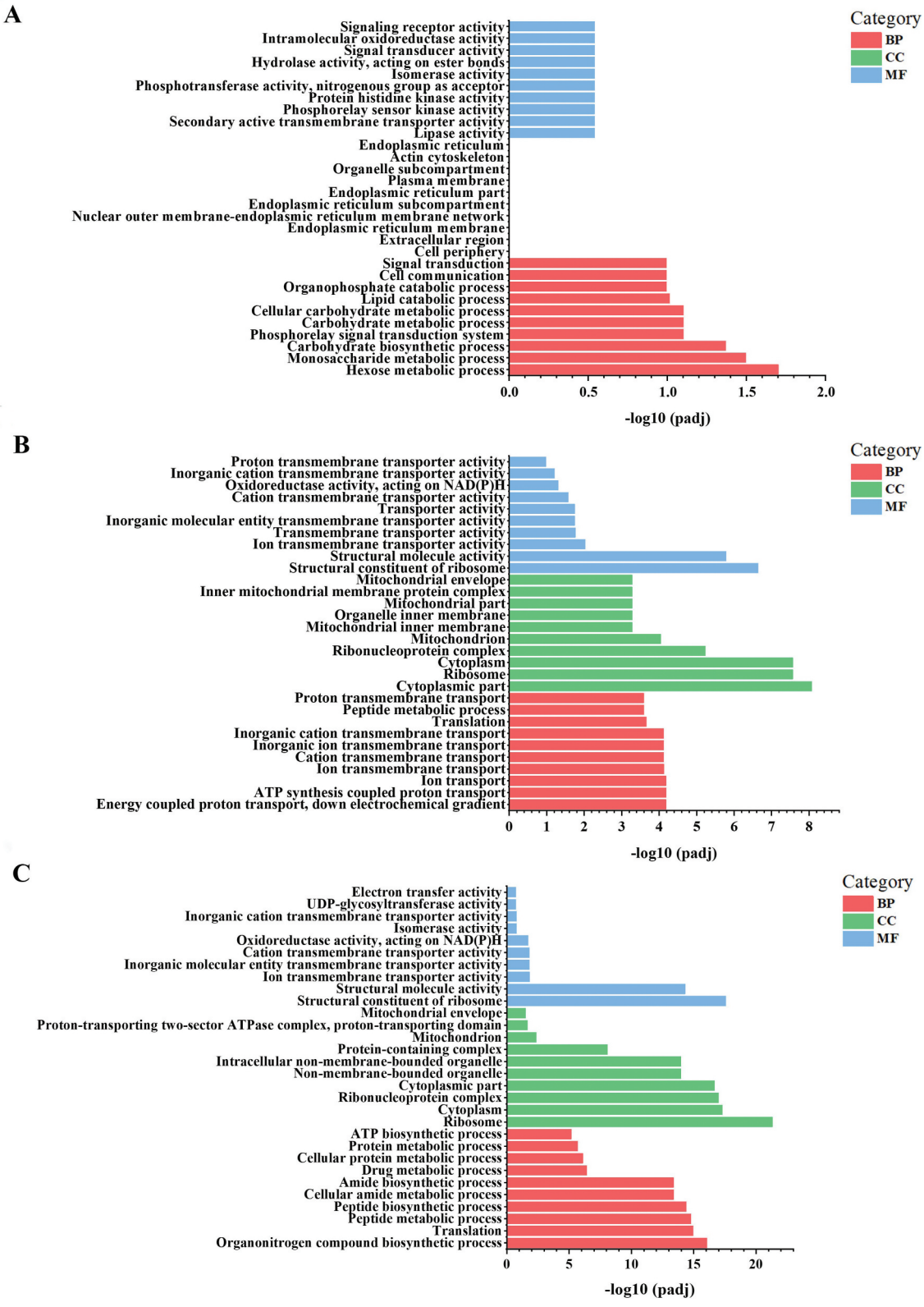

Figure 3. GO functional analysis of differential genes. (A) GO function classification under 20 g/L NaCl vs. 0 g/L NaCl. (B) 100 g/L NaCl vs. 0 g/L NaCl. (C) 100 g/L NaCl vs. 20 g/L NaCl. The horizontal axis represents GO terms, and the vertical axis indicates the significance of GO term enrichment. Different colours represent BP (biological process), CC (cellular component), and MF (molecular function). GO enrichment is considered significant when padj < 0.05.

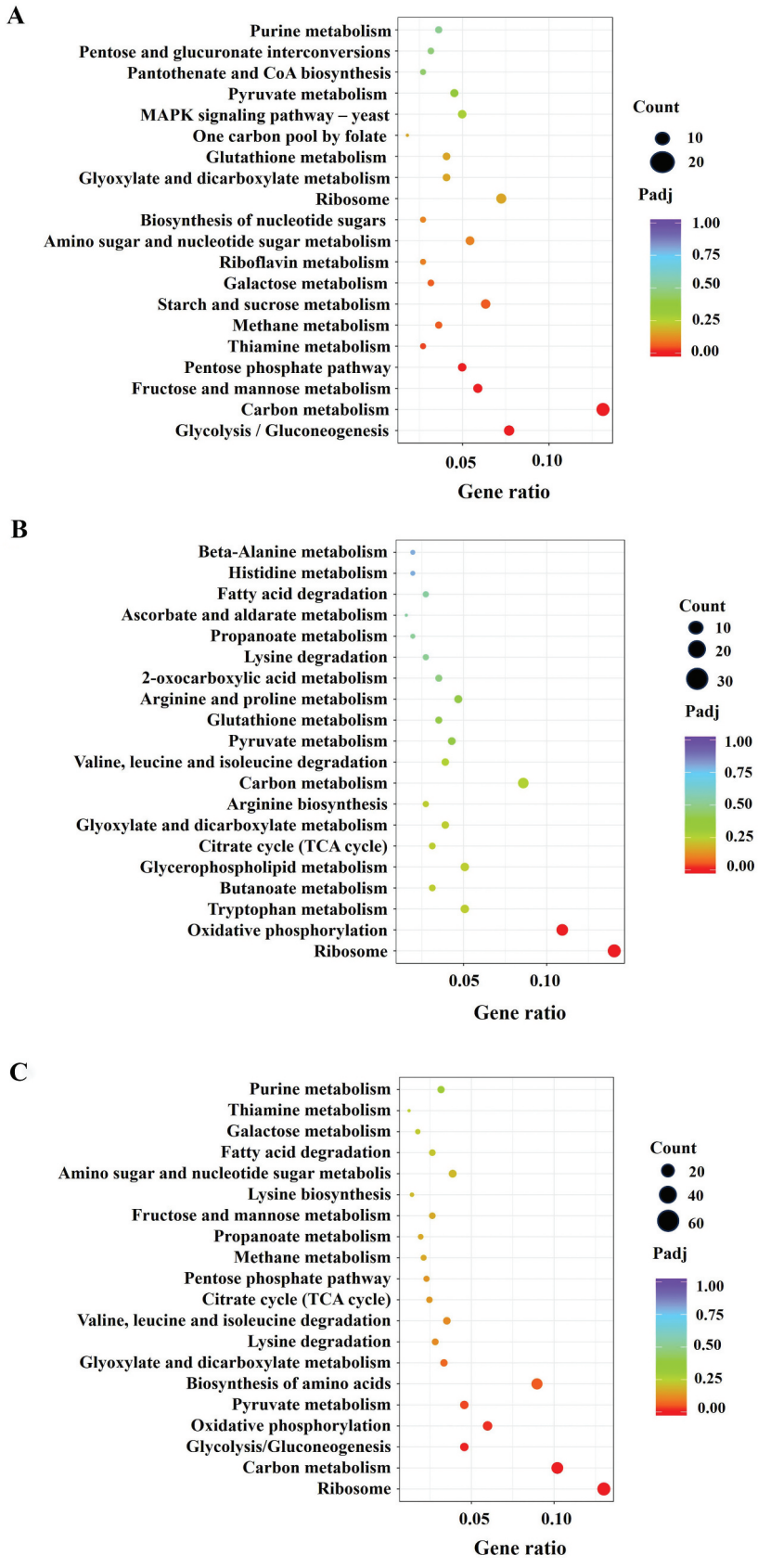

Figure 4. KEGG functional analysis of differential genes. (A) KEGG-enriched pathways for 20 g/L NaCl vs. 0 g/L NaCl. (B) 100 g/L NaCl vs. 0 g/L NaCl. (C) 100 g/L NaCl vs. 20 g/L NaCl. The horizontal axis shows the ratio of annotated differential genes, and the vertical axis indicates the KEGG pathway. Dot size reflects the number of annotated genes, while colour (red to purple) indicates enrichment significance.

amino acid biosynthesis pathway (Figure 4C). Comparing NaCl concentrations, Glycolysis, Carbon Metabolism, and MAPK Signaling were significant at 20 g/L, while the ribosomal, oxidative phosphorylation, and carbon metabolism pathways were highly enriched at 100 g/L.

3.4. HOG-MAPK pathway differential gene analysis

The results of the KEGG pathway-enriched *HOG*-MAPK pathway are shown in Figure 5. Among them, KEGG nodes containing up-regulated genes are labelled in red, and KEGG nodes containing down-regulated genes are labelled in green. Comparison of the experimental group (20 g/L NaCl) with the control group (0 g/L NaCl) showed Figure 5A that one gene encoding for an article (*Ste50*) was upregulated and four genes encoding for phosphotransfer protein genes (*Ypd1*), mitogen-activated protein kinase genes (*HOG1*), protein tyrosine phosphatase genes (*Ptp2*, *Ptp3*). Comparison of the experimental group (100 g/L NaCl) with the control group (0 g/L NaCl) showed that the four coding genes of *HOG*-MAPK pathway were up-regulated in Figure 5B were glycerol synthase gene (*Gpd1*), small chromosome maintenance protein 1 gene (*Mcm1*), catalase gene (*Ctt1*), and *HOG1* in which mitogen-activated protein kinase gene encoding gene was significantly up-regulated. Two coding genes were down-regulated for MAP3K (*Ste11*) and type 2C protein phosphatase gene (*Ptc1*). Comparison of the experimental group (100 g/L NaCl) with the control group (20 g/L NaCl) showed that 4 coding genes in the *HOG*-MAPK pathway were up-regulated in Figure 5C as *Gpd1*, *Mcm1*, *Ctt1*, and *HOG1* respectively, among which *Ctt1* and *HOG1* genes were significantly up-regulated. Two coding genes were down-regulated *Ptc1* and tyrosine-protein kinase gene (*Swe1*).

3.5. OTA biosynthetic genes and HOG1 gene expression under different osmolarity conditions

The qRT-PCR analysis revealed the expression of OTA biosynthesis genes (*otaA–D*) and the *HOG1* gene. The results indicated that the transcript expression level of the *HOG1* gene decreased by 78.06%. When the NaCl concentration was 20 g/L compared to 0 g/L NaCl. When the NaCl concentration was 100 g/L, the transcript expression level of the *HOG1* gene increased by 28.32% compared to 0 g/L NaCl. Additionally, the OTA synthesis genes (*otaA*, *otaB*, *otaC*, and *otaD*) showed increases of 3.26-fold, 1.99-fold, 2.06-fold, and 0.41-fold, respectively, at 20 g/L NaCl compared to 0 g/L NaCl. The up-regulation of the *otaD* gene was particularly notable, showing a 6.49-fold increase under the 100 g/L NaCl culture condition compared to the 0 g/L NaCl condition (Figure 6).

4. Discussion

In this study, RNA-Seq technology was used to investigate genes that are expressed differently and conducted a KEGG pathway analysis of the *A. westerdijkiae* fc-1 strain under conditions with 0, 20, and 100 g/L of NaCl. Similarly, genes involved in glycerol accumulation, sugar metabolism, organic acid storage, pigment production, and asexual spore formation in *A. westerdijkiae* are regulated differently in response to salt stress (Liu et al. 2017). Significant changes in genes involved in the process of sugar metabolism in *A. westerdijkiae* fc-1 under 20 g/L NaCl versus 0 g/L NaCl concentration and in the *HOG* pathway (tyrosine protein phosphatase, *Ptp2,3*) involved in the regulation of meiosis and sporulation were observed as a result of the consistency of present findings. A study reported that genes differentially expressed by *Aspergillus montevidensis* ZYD4 under high salt concentration conditions are involved in regulating amino acid, metabolism, ion transport, saturated fatty acid synthesis, fatty acid β-oxidation, oxidative stress tolerance, and soluble sugar accumulation electron transport (Ding et al. 2019). Consistent with the present study's findings, *A. westerdijkiae* fc-1 exhibited significant changes in genes related to ion transport, ion transmembrane translocation and those encoding proteins involved in carbohydrate and lipid metabolism in the *HOG* pathway under 100 g/L NaCl compared to 0 g/L NaCl conditions. The goal was to achieve a more comprehensive and accurate understanding of the pathways involved in OTA production and their regulatory mechanisms.

The change in NaCl concentration resulted in substantial transcriptional changes in an enormous number of genes. GO functional classification and KEGG enrichment analysis of DEGs revealed significant

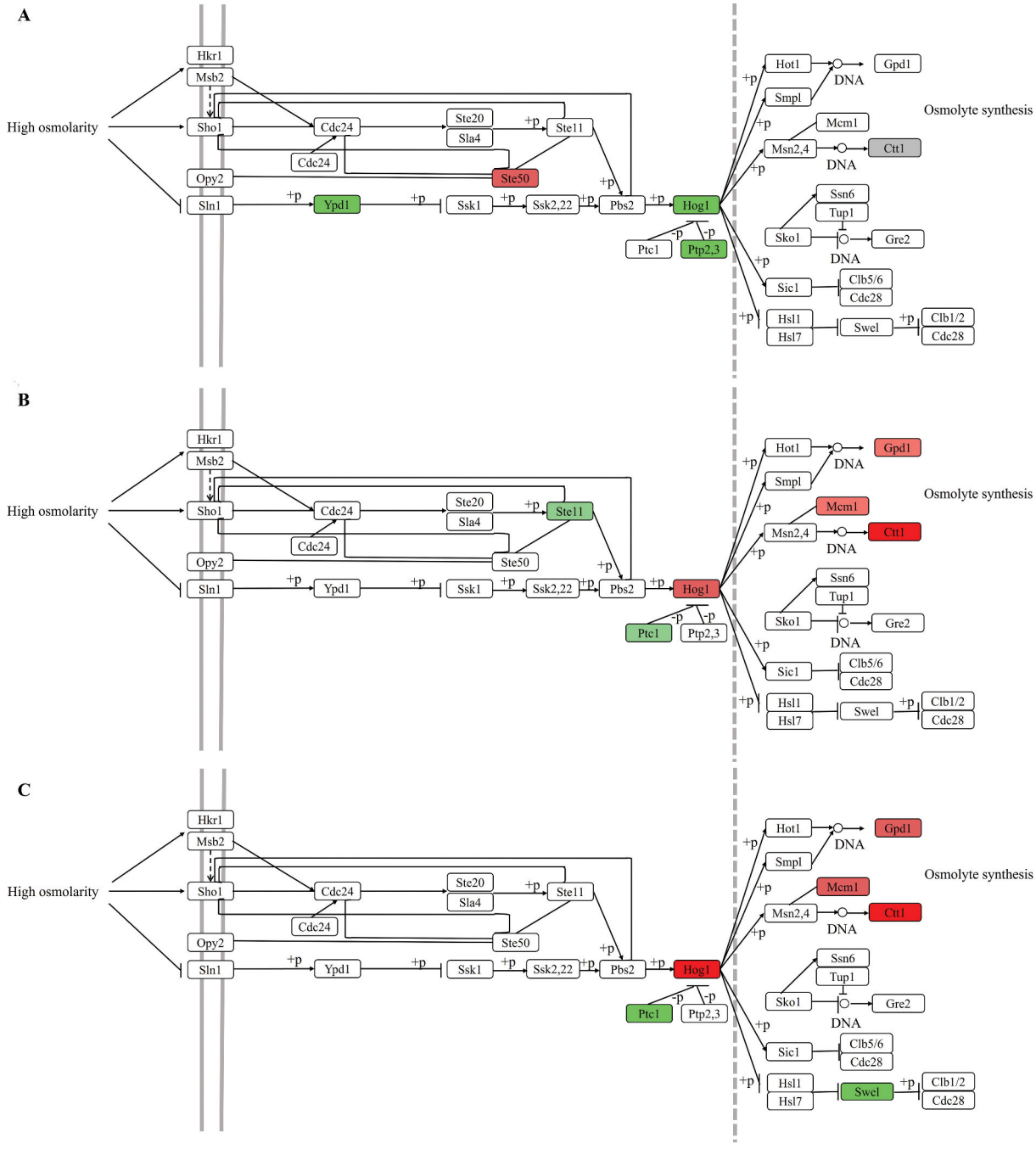

Figure 5. Differential gene analysis of the *HOG*-MAPK pathway. (A) Gene changes under 20 g/L NaCl vs. 0 g/L NaCl. (B) 100 g/L NaCl vs. 0 g/L NaCl. (C) 100 g/L NaCl vs. 20 g/L NaCl. Up-regulated genes are in red, down-regulated genes are in green, with colour intensity indicating significance.

changes in carbohydrate metabolism pathways when the NaCl concentration reached 20 g/L compared to 0 g/L. This concentration may be more suitable for *A. westerdijkiae* fc-1, as it appears to stimulate OTA biosynthesis. The enzyme *otaD* helps maintain intracellular chloride ion homoeostasis by excreting chloride-bound OTA molecules. This suggests that the *Aspergillus* species involved in producing OTA can sense and react to NaCl concentration changes in their environment to regulate OTA production (Wei et al. 2022; Wang et al. 2023). The increased number of cellular communication and signalling-enriched differential genes may be the result of the *A. westerdijkiae* receiving NaCl as an environmental signal to regulate its mycelium growth, and metabolism (Corrochano et al. 2016). Up-regulated DEGs,

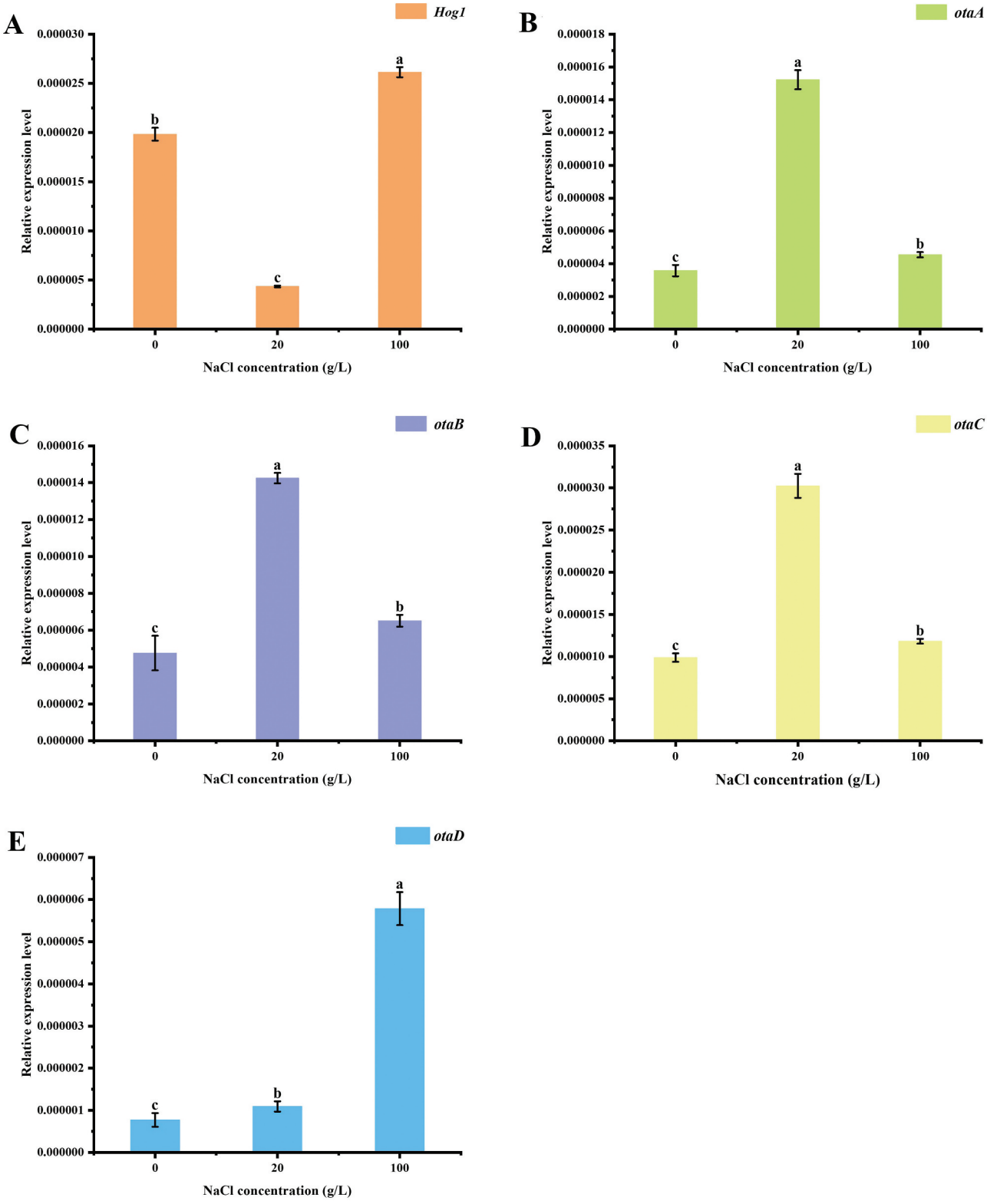

Figure 6. The relative levels of gene expression of *Hog1* (A) and OTA biosynthesis genes, *otaA* (B), *otaB* (C), *otaC* (D), and *otaD* (E) under different NaCl concentration. Different letters (a, b, c) in each subfigure indicate significant differences between the corresponding values ($p < 0.05$).

including genes for hydrolases and isoenzymes play a hydrolytic role in sugar metabolism, generating malonate and acetic acid as feedstock for PKS and meeting the nutritional requirements of the fungus (Rafiei et al. 2021; Nam 2022). Upregulation expression of genes related to the glyoxylate and dicarboxylic acid metabolic pathways could be a crucial factor in the accumulation of metabolites in fungi (Lorenz and Fink 2001; Ostachowska et al. 2017).

The GO functional classification and KEGG enrichment study of DEGs revealed significant changes in differentially expressed genes related to ion transport and ion transmembrane transporter activity when the NaCl concentration reached 100 g/L compared to 0 g/L. This change is likely attributed to the substantial increase in Na^+ and Cl^- concentrations. The elevated ion levels may have accelerated the rate of ion transport and enhanced transporter protein activity (Wang et al. 2023). The substantial rise in the number of differential genes in cellular components; mitochondria, ribosomes and cytoplasmic differential genes may be due to high osmotic stress disruption in *A. westerdijkiae* fc-1 strain. The upregulation of oxidative phosphorylation pathway differential genes may be due to the active transport of ions that requires oxidative phosphorylation for ATP synthesis (Lavín et al. 2013). The increase in ribosomal pathway differential genes may be an alteration in the efficiency of synthesised proteins (Mullis et al. 2020). When NaCl concentration reached 100 g/L compared to 20 g/L, GO functional classification and KEGG enrichment pathway analysis in up-regulated genes showed significant elevation of ribosomal and amino acid metabolic pathways. Amino acids have been reported to be important components of proteins and secondary metabolites in different fungal species (Steyer et al. 2023). The higher enrichment of carbon metabolism and pyruvate metabolism pathway genes may be the function of *A. westerdijkiae* fc-1 strain to carry out the synthesis of secondary metabolites as well as its aerobic respiration (Chroumpi et al. 2020).

Recent studies have demonstrated that the MAPK cascade, a central element of the *HOG*-MAPK pathway, is highly conserved. This cascade is composed of a tri-kinase module, including MAP3K, MAP2K and MAPK (Ma and Li 2013). In response to osmotic stress, two independent upstream osmotic sensing mechanisms, the Sln1 and Sho1 branches, are activated. These mechanisms trigger specific MAP3Ks, Ssk2/22 and Ste11, respectively. Both MAP3Ks colocalize on the common Pbs2 MAP2K. Once activated, Pbs2 phosphorylates the *HOG1* MAPK, which then initiates a series of adaptive responses (Dexter et al. 2015; de Nadal and Posas 2022). The mucin-like transmembrane proteins Hkr1 and Msb2 act as potential osmo-sensors in the SHO1 branch and found that Hkr1 and Msb2 alone form a complex with Sho1, inducing intracellular signalling from Sho1 under high external osmotic stress (Tatebayashi et al. 2007). Additionally, Sho1 homo-oligomers which are four-transmembrane permeability sensors, interact with the transmembrane co-permeability sensors Hkr1 and Msb2, as well as the membrane-anchoring protein Opy2, through their transmembrane structural domains. This interaction activates the Ste20-Ste11-Pbs2-*HOG1* kinase cascade (Takayama et al. 2019).

However, genes in the *HOG*-MAPK pathway changed significantly under different osmolarity conditions (Ma et al. 2024). The results of the *HOG*-MAPK pathway differential gene analysis showed that the gene encoding Ste50 was up-regulated in the *A. westerdijkiae* fc-1 strain at 20 g/L NaCl compared to 0 g/L NaCl. The report suggests that in *Saccharomyces cerevisiae*, Ste50 plays a role in cellular signalling between activated G proteins and MAP3K Ste11, especially during periods of increased signalling activity in *S. cerevisiae* (Ramezani-Rad 2003). MAP3K Ste11 is involved in transmitting signals between the G protein and itself, possibly during times of increased signalling activity in this yeast (Ikunaga et al. 2011). The genes coding for *Ypd1*, *HOG1*, *Ptp2*, and *Ptp3* were down-regulated, and the deletion of *Ptp2*, and *Ptp3*, which are reported to be involved in the regulation of meiosis and sporulation, resulted in a defect in sporulation possibly when the concentration of 20 g/L NaCl was not optimal concentration for spore formation in *A. westerdijkiae* fc-1 strain (Zhan et al. 2000). The down-regulation of genes encoding *Ypd1* and *HOG1* may be due to the fact that a concentration of 20 g/L NaCl is within normal growth conditions. The three-component phosphorelay system, consisting of the histidine kinase *Sln1*, the transfer protein *Ypd1*, and the response regulator *Ssk1*, likely inhibits the *HOG* pathway under these conditions. This inhibition occurs through the phosphorylation of *Ssk1*, which suppresses *HOG* pathway activity. These

findings suggest that the *HOG* pathway may not be activated at this NaCl concentration (Dexter et al. 2015).

Genes encoding for *Gpd1*, *Mcm1*, *Ctt1*, and *HOG1* were up-regulated in *A. westerdijkiae* fc-1 strain at 100 g/L compared with 0 g/L NaCl, with the gene encoding for *Ctt1* being significantly up-regulated. The up-regulation of the gene encoding for *HOG1* may be the result of activation of the *HOG* pathway under 100 g/L NaCl conditions. The *Gpd1* (3-phosphoglycerol dehydrogenase) encoding gene has been reported to be involved in lipid metabolism, carbohydrate and provides protection against osmotic and hypoxic stress in *S. cerevisiae* possibly indicating activation of the *HOG*-pathway in response to high osmotic pressure environment for self-protection at a concentration of 100 g/L NaCl (Alarcon et al. 2012). The *Mcm1* encoding gene can protect against impaired cellular integrity, cell wall structural distortion, and altered cell wall composition may indicate that the expression of the strain was upregulated at 100 g/L NaCl concentration to maintain its cellular integrity (Zhao et al. 2019). *Ctt1* encoding genes have an important role in cross-protection against osmotic stress (Schüller et al. 1994). Genes encoding for *Ste11* and Ptc*1* were downregulated, as *Ste11* was activated during the high osmotic glycerol pathway activation is stabilised during the period. Since the steady-state amount of *Ste11* does not change significantly during pheromone induction, it can be hypothesised that the pheromone induction process in *A. westerdijkiae* fc-1 strain is inhibited at 100 g/L NaCl concentration (Ramezani-Rad 2003). It has been reported that the deletion of the Ptc1 iso-coding gene leads to delayed mitochondrial transport but does not block it completely thus it is hypothesised that the down-regulation of the *Ptc1* gene may be responsible for the inhibitory effect of mitochondrial transport of the strain at 100 g/L NaCl thus affecting its growth (Roeder et al. 1998). When 100 g/L was compared with 20 g/L NaCl. The results of the *HOG*-MAPK pathway differential gene analysis were consistent with the expression of the majority of the encoded genes at 100 g/L versus 0 g/L NaCl. The difference was that the Swe1-encoded genes were down-regulated. In contrast, the Ste11 genes were not significantly changed, and the *Δswe1* mutant was reported to be smaller than wild-type cells, which led to the speculation that the down-regulation of the Swe1-encoded genes might delay the cell cycle and reduce the cell size (McNulty and Lew 2005).

The expression of OTA biosynthesis genes (*otaA–D*) and *HOG1* genes of *A. westerdijkiae* fc-1 strain was correlated with OTA biosynthesis with different concentrations of NaCl as detected by qRT-PCR (Wang et al. 2020). Changes in the expression of OTA biosynthesis genes (*otaA–D*) play a crucial role in regulating OTA production. At a NaCl concentration of 20 g/L, the *HOG1* gene was down-regulated in the *A. westerdijkiae* fc-1 strain leading to a significant increase in the expression of the *otaA-C* biosynthesis genes. This increase was positively correlated which can be associated with higher OTA production as compared to the control group (0 g/L NaCl). These results suggest that *A. westerdijkiae* fc-1 is more efficient at synthesising OTA under elevated NaCl concentrations. Further transcriptome analysis revealed significant changes in pathways related to carbohydrate metabolism, hydrolytic enzyme synthesis, and the metabolism of acetaldehyde and dicarboxylic acids indicating that these metabolic processes may also be closely linked to OTA production. At a higher NaCl concentration of 100 g/L, the *HOG1* gene was up-regulated, which resulted in a marked increase in the expression of the *otaD* biosynthesis gene. However, the expression of *otaA-C* was only slightly increased and showed a negative correlation which can be associated with OTA production. This pattern suggests that when the *HOG* pathway is activated, possibly as a protective mechanism, OTA production may be significantly inhibited. These findings highlight key genes and pathways involved in OTA biosynthesis and offer a broader context for understanding the molecular mechanisms underlying OTA production in *A. westerdijkiae* fc-1 under specific environmental conditions. When the concentration of NaCl was 100 g/L compared to 20 g/L, the expression of the *HOG1* gene was significantly up-regulated but the expression of OTA synthesis genes (*otaA–C*) was lower than that of 20 g/L (*otaA–C*), which may indicate that the expression of OTA biosynthesis genes (*otaA–D*) and *HOG1* genes are not positively correlated (Stoll et al. 2013). *otaD* genes in the OTA synthesis pathway are responsible for introducing chloride ions at the chlorination step (Ferrara et al. 2016). The up-regulation of expression may be due to the high Cl^- concentration at this point to maintain partial intracellular Cl^- homoeostasis (Wang et al. 2018). In this study, transcriptome analysis of key metabolic pathways

and differential genes in the *A. westerdijkiae* fc-1 strain under varying osmotic pressure conditions was combined with OTA production data to gain a precise understanding of the molecular pathways involved in OTA production. The findings can be applied to develop strategies for controlling OTA contamination in the food and agricultural industries. This research provides a theoretical foundation for future studies on specific genes and metabolic pathways and can contribute to the development of molecular markers for monitoring OTA contamination levels. The broader implications of these results include improving food safety and understanding the environmental factors that influence OTA biosynthesis.

5. Conclusions

This research employed RNA sequencing technology to identify differentially expressed genes in *A. westerdijkiae* fc-1 strain under varying osmotic pressure conditions. Through an in-depth analysis, particularly of the *HOG* pathway, significant pathways were uncovered. A connection was also established between the altered gene expression within the *HOG* pathway and OTA production. These findings lay the groundwork for developing strategies to reduce OTA contamination in foodstuffs.

Author contributions

Methodology, Y.M. and M.Z.; formal analysis, G.T. and Y.D.; validation, Y.M, T.A. and M.L.; writing and original draft preparation, M.Z, and Y.M.; writing, review and editing, Y.L., T.A, Y.M., and M.Z.; project administration, T.A. and Y.L.; funding acquisition, Y.L.

Disclosure statement

No potential conflict of interest was reported by the author(s).

Funding

The work was supported by Guangdong Basic and Applied Basic Research Foundation [2022A1515010037], and the National Key Research and Development Program of China [2022YFE0139500].

References

Alarcon DA, Nandi M, Carpena X, Fita I, Loewen PC. 2012. Structure of glycerol-3-phosphate dehydrogenase (GPD1) from *Saccharomyces cerevisiae* at 2.45 Å resolution. Acta Crystallogr Sect F Struct Biol Cryst Commun. 68(Pt 11):1279–1283. doi: 10.1107/S1744309112037736.

Altafini A, Fedrizzi G, Roncada P. 2019. Occurrence of ochratoxin a in typical salami produced in different regions of Italy. Mycotoxin Res. 35(2):141–148. doi: 10.1007/s12550-018-0338-x.

Anli E, Alkis İM. 2010. Ochratoxin a and brewing technology: a review. J I Brew. 116(1):23–32. doi: 10.1002/j.2050-0416.2010.tb00394.x.

Bai Y, Wang J, Han J, Xie XL, Ji CG, Yin J, Chen L, Wang CK, Jiang XY, Qi W, et al. 2017. BCL2L10 inhibits growth and metastasis of hepatocellular carcinoma both *in vitro* and *in vivo*. Mol Carcinog. 56(3):1137–1149. doi: 10.1002/mc.22580.

Cabañas R, Bragulat MR, Abarca ML, Castellá G, Cabañes FJ. 2008. Occurrence of *Penicillium verrucosum* in retail wheat flours from the Spanish market. Food Microbiol. 25 (5):642–647. doi: 10.1016/j.fm.2008.04.003.

Cabañes FJ, Bragulat MR, Castellá G. 2010. Ochratoxin a producing species in the genus *Penicillium*. Toxins (Basel). 2(5):1111–1120. doi: 10.3390/toxins2051111.

Chen Y, Chen J, Zhu Q, Wan J. 2022. Ochratoxin a in dry-cured ham: OTA-producing fungi, prevalence, detection methods, and biocontrol strategies-a review. Toxins (Basel). 14 (10):693. doi: 10.3390/toxins14100693.

Chroumpi T, Mäkelä MR, de Vries RP. 2020. Engineering of primary carbon metabolism in filamentous fungi. Biotechnol Adv. 43:107551. doi: 10.1016/j.biotechadv.2020.107551.

Corrochano LM, Kuo A, Marcet-Houben M, Polaino S, Salamov A, Villalobos-Escobedo JM, Grimwood J, Álvarez MI, Avalos J, Bauer D, et al. 2016. Expansion of signal transduction pathways in fungi by extensive genome duplication. Curr Biol. 26(12):1577–1584. doi: 10.1016/j.cub.2016.04.038.

de Nadal E, Posas F. 2022. The *HOG* pathway and the regulation of osmoadaptive responses in yeast. FEMS Yeast Res. 22(1): foac013. doi: 10.1093/femsyr/foac013.

Dexter JP, Xu P, Gunawardena J, McClean MN. 2015. Robust network structure of the Sln1-Ypd1-Ssk1 three-component phospho-relay prevents unintended activation of the *HOG* MAPK pathway in *Saccharomyces cerevisiae*. BMC Syst Biol. 9 (1):17. doi: 10.1186/s12918-015-0158-y.

Ding X, Liu K, Lu Y, Gong G. 2019. Morphological, transcriptional, and metabolic analyses of osmotic-adapted mechanisms of the halophilic *Aspergillus montevidensis* ZYD4 under hypersaline conditions. Appl Microbiol Biotechnol. 103 (9):3829–3846. doi: 10.1007/s00253-019-09705-2.

Ferrara M, Perrone G, Gambacorta L, Epifani F, Solfrizzo M, Gallo A, Brakhage AA. 2016. Identification of a halogenase

involved in the biosynthesis of ochratoxin a in *Aspergillus carbonarius*. Appl Environ Microbiol. 82(18):5631–5641. doi: 10.1128/AEM.01209-16.

Gallo A, Ferrara M, Perrone G. 2013. Phylogenetic study of polyketide synthases and nonribosomal peptide synthetases involved in the biosynthesis of mycotoxins. Toxins (Basel). 5(4):717–742. doi: 10.3390/toxins5040717.

Gallo A, Knox BP, Bruno KS, Solfrizzo M, Baker SE, Perrone G. 2014. Identification and characterization of the polyketide synthase involved in ochratoxin a biosynthesis in *Aspergillus carbonarius*. Int J Food Microbiol. 179:10–17. doi: 10.1016/j.ijfoodmicro.2014.03.013.

Geisen R, Mayer Z, Karolewiez A, Färber P. 2004. Development of a real time PCR system for detection of *Penicillium nordicum* and for monitoring ochratoxin a production in foods by targeting the ochratoxin polyketide synthase gene. Syst Appl Microbiol. 27(4):501–507. doi: 10.1078/0723202041438419.

Gerin D, De Miccolis Angelini RM, Pollastro S, Faretra F, Sarrocco S. 2016. RNA-Seq reveals OTA-related gene transcriptional changes in *Aspergillus carbonarius*. PLOS One. 11(1):e0147089. doi: 10.1371/journal.pone.0147089.

Hesseltine CW, Vandegraft EE, Fennell DI, Smith ML, Shotwell OL. 1972. Aspergilli as ochratoxin producers. Mycologia. 64(3):539–550. doi: 10.1080/00275514.1972.12019299.

Hussein MA, Gherbawy YA, El-Sadek MSA, Al-Harthi HF, El-Dawy EG. 2024. Phylogeny of *Aspergillus* section *Circumdati* and inhibition of ochratoxins potential by green synthesised ZnO nanoparticles. Mycology. 1–12. doi: 10.1080/21501203.2024.2379480.

Ikunaga Y, Sato I, Grond S, Numaziri N, Yoshida S, Yamaya H, Hiradate S, Hasegawa M, Toshima H, Koitabashi M, et al. 2011. *Nocardioides* sp. strain WSN05-2, isolated from a wheat field, degrades deoxynivalenol, producing the novel intermediate 3-epi-deoxynivalenol. Appl Microbiol Biotechnol. 89(2):419–427. doi: 10.1007/s00253-010-2857-z.

Lamarre C, Sokol S, Debeaupuis JP, Henry C, Lacroix C, Glaser P, Coppée JY, François JM, Latgé JP. 2008. Transcriptomic analysis of the exit from dormancy of *Aspergillus fumigatus* conidia. BMC Genom. 9(1):417. doi: 10.1186/1471-2164-9-417.

Lavín JL, Marcet-Houben M, Gutiérrez-Vázquez RL, Ramírez L, Pisabarro AG, Gabaldón T, Oguiza JA. 2013. FUNGALOXPHOS: an integrated database for oxidative phosphorylation in fungi. Mitochondrion. 13(4):357–359. doi: 10.1016/j.mito.2013.04.009.

Liu KH, Ding XW, Narsing Rao MP, Zhang B, Zhang YG, Liu FH, Liu BB, Xiao M, Li WJ. 2017. Morphological and transcriptomic analysis reveals the osmoadaptive response of endophytic fungus *Aspergillus montevidensis* ZYD4 to high salt stress. Front Microbiol. 8:1789. doi: 10.3389/fmicb.2017.01789.

Lorenz MC, Fink GR. 2001. The glyoxylate cycle is required for fungal virulence. Nature. 412(6842):83–86. doi: 10.1038/35083594.

Ma D, Li R. 2013. Current understanding of *HOG*-MAPK pathway in *Aspergillus fumigatus*. Mycopathologia. 175(1–2):13–23. doi: 10.1007/s11046-012-9600-5.

Ma Y, Li M, Ahmad T, Deng Y, Zhuang M, Tan G, Liu Y. 2024. Impact of *OTAbZIP* on ochratoxin a production, mycelium growth and pathogenicity of *Aspergillus westerdijkiae* under water activity stress. Mycology. 8(9):1–11. doi: 10.1080/21501203.2024.2355333.

McNulty JJ, Lew DJ. 2005. Swe1p responds to cytoskeletal perturbation, not bud size, in *S. cerevisiae*. Curr Biol. 15(24):2190–2198. doi: 10.1016/j.cub.2005.11.039.

Mullis A, Lu Z, Zhan Y, Wang TY, Rodriguez J, Rajeh A, Chatrath A, Lin Z, Russo C. 2020. Parallel concerted evolution of ribosomal protein genes in fungi and its adaptive significance. Mol Biol Evol. 37(2):455–468. doi: 10.1093/molbev/msz229.

Nam KH. 2022. Glucose isomerase: functions, structures, and applications. Appl Sci. 12(1):428. doi: 10.3390/app12010428.

Navale V, Vamkudoth KR, Ajmera S, Dhuri V. 2021. *Aspergillus* derived mycotoxins in food and the environment: prevalence, detection, and toxicity. Toxicol Rep. 8:1008–1030. doi: 10.1016/j.toxrep.2021.04.013.

Novodvorska M, Hayer K, Pullan ST, Wilson R, Blythe MJ, Stam H, Stratford M, Archer DB. 2013. Transcriptional landscape of *Aspergillus niger* at breaking of conidial dormancy revealed by RNA-sequencing. BMC Genom. 14(1):246. doi: 10.1186/1471-2164-14-246.

O'Callaghan J, Caddick MX, Dobson ADW. 2003. A polyketide synthase gene required for ochratoxin a biosynthesis in *Aspergillus ochraceus*. Microbiology. 149(12):3485–3491. doi: 10.1099/mic.0.26619-0.

O'Callaghan J, Coghlan A, Abbas A, García-Estrada C, Martín J-F, Dobson ADW. 2013. Functional characterization of the polyketide synthase gene required for ochratoxin a biosynthesis in *Penicillium verrucosum*. Int J Food Microbiol. 161(3):172–181. doi: 10.1016/j.ijfoodmicro.2012.12.014.

Ostachowska A, Stepnowski P, Gołębiowski M. 2017. Dicarboxylic acids and hydroxy fatty acids in different species of fungi. Chem Pap. 71(5):999–1005. doi: 10.1007/s11696-016-0008-4.

Parkhomchuk D, Borodina T, Amstislavskiy V, Banaru M, Hallen L, Krobitsch S, Lehrach H, Soldatov A. 2009. Transcriptome analysis by strand-specific sequencing of complementary DNA. Nucleic Acids Res. 37(18):e123. doi: 10.1093/nar/gkp596.

Pyo MC, Choi IG, Lee KW. 2021. Transcriptome analysis reveals the AhR, Smad2/3, and HIF-1α pathways as the mechanism of ochratoxin a toxicity in kidney cells. Toxins (Basel). 13(3):190. doi: 10.3390/toxins13030190.

Rafiei V, Vélëz H, Tzelepis G. 2021. The role of glycoside hydrolases in phytopathogenic fungi and oomycetes virulence. Int J Mol Sci. 22(17):9359. doi: 10.3390/ijms22179359.

Ramezani-Rad M. 2003. The role of adaptor protein Ste50-dependent regulation of the MAPKKK Ste11 in multiple signalling pathways of yeast. Curr Genet. 43(3):161–170. doi: 10.1007/s00294-003-0383-6.

Roeder AD, Hermann GJ, Keegan BR, Thatcher SA, Shaw JM. 1998. Mitochondrial inheritance is delayed in *Saccharomyces cerevisiae* cells lacking the serine/threonine phosphatase PTC1. Mol Biol Cell. 9(4):917–930. doi: 10.1091/mbc.9.4.917.

Schmidt-Heydt M, Graf E, Batzler J, Geisen R. 2011. The application of transcriptomics to understand the ecological reasons of ochratoxin a biosynthesis by *Penicillium nordicum* on sodium chloride rich dry cured foods. Trends Food Sci Tech. 22:S39–S48. doi: 10.1016/j.tifs.2011.02.010.

Schmidt-Heydt M, Graf E, Stoll D, Geisen R. 2012. The biosynthesis of ochratoxin a by *Penicillium* as one mechanism for adaptation to NaCl rich foods. Food Microbiol. 29 (2):233–241. doi: 10.1016/j.fm.2011.08.003.

Schüller C, Brewster JL, Alexander MR, Gustin MC, Ruis H. 1994. The *HOG* pathway controls osmotic regulation of transcription via the stress response element (STRE) of the *Saccharomyces cerevisiae* CTT1 gene. Embo J. 13 (18):4382–4389. doi: 10.1002/j.1460-2075.1994.tb06758.x.

Steyer JT, Todd RB, Jones G, Usher J. 2023. Branched-chain amino acid biosynthesis in fungi. Essays Biochem. 67 (5):865–876. doi: 10.1042/EBC20230003.

Stoll D, Schmidt-Heydt M, Geisen R. 2013. Differences in the regulation of ochratoxin a by the *HOG* pathway in *Penicillium* and *Aspergillus* in response to high osmolar environments. Toxins (Basel). 5(7):1282–1298. doi: 10.3390/toxins5071282.

Takayama T, Yamamoto K, Saito H, Tatebayashi K, Sugiura R. 2019. Interaction between the transmembrane domains of Sho1 and Opy2 enhances the signaling efficiency of the *HOG1* MAP kinase cascade in *Saccharomyces cerevisiae*. PLOS One. 14(1):e0211380. doi: 10.1371/journal.pone.0211380.

Tatebayashi K, Tanaka K, Yang HY, Yamamoto K, Matsushita Y, Tomida T, Imai M, Saito H. 2007. Transmembrane mucins Hkr1 and Msb2 are putative osmosensors in the SHO1 branch of yeast *HOG* pathway. Embo J. 26(15):3521–3533. doi: 10.1038/sj.emboj.7601796.

Vipotnik Z, Rodríguez A, Rodrigues P. 2017. *Aspergillus westerdijkiae* as a major ochratoxin a risk in dry-cured ham based-media. Int J Food Microbiol. 241:244–251. doi: 10.1016/j.ijfoodmicro.2016.10.031.

Wang G, Li E, Gallo A, Perrone G, Varga E, Ma J, Yang B, Tai B, Xing F. 2023. Impact of environmental factors on ochratoxin A: from natural occurrence to control strategy. Environ Pollut. 317:120767. doi: 10.1016/j.envpol.2022.120767.

Wang L, Wang Y, Wang Q, Liu F, Selvaraj JN, Liu L, Xing F, Zhao Y, Zhou L, Liu Y. 2015. Functional characterization of new polyketide synthase genes involved in ochratoxin a biosynthesis in *Aspergillus ochraceus* fc-1. Toxins (Basel). 7 (8):2723–2738. doi: 10.3390/toxins7082723.

Wang YF, Liu F, Pei J, Yan H, Wang Y. 2023. The Aw*HOG1* transcription factor influences the osmotic stress response, mycelium growth, OTA production, and pathogenicity in *Aspergillus westerdijkiae* fc-1. Toxins (Basel). 15(7):432. doi: 10.3390/toxins15070432.

Wang YH, Dong F, Chen H, Xu T, Tang M. 2023. Effects of arbuscular mycorrhizal fungus on sodium and chloride ion channels of *Casuarina glauca* under salt stress. Int J Mol Sci. 24(4):3680. doi: 10.3390/ijms24043680.

Wang Y, Wang L, Liu F, Wang Q, Selvaraj JN, Xing F, Zhao Y, Liu Y. 2016. Ochratoxin a producing fungi, biosynthetic pathway and regulatory mechanisms. Toxins (Basel). 8 (3):83. doi: 10.3390/toxins8030083.

Wang Y, Wang L, Wu F, Liu F, Wang Q, Zhang X, Selvaraj JN, Zhao Y, Xing F, Yin WB, et al. 2018. A consensus ochratoxin a biosynthetic pathway: insights from the genome sequence of *Aspergillus ochraceus* and a comparative genomic analysis. Appl Environ Microbiol. 84(19):e01009-18. doi: 10.1128/AEM.01009-18.

Wang Y, Yan H, Neng J, Gao J, Yang B, Liu Y. 2020. The influence of NaCl and glucose content on growth and ochratoxin a production by *Aspergillus ochraceus, Aspergillus carbonarius and Penicillium nordicum, Aspergillus carbonarius* and *Penicillium nordicum*. Toxins. 12(8):515. doi: 10.3390/toxins12080515.

Wei S, Hu C, Nie P, Zhai H, Zhang S, Li N, Lv Y, Hu Y. 2022. Insights into the underlying mechanism of ochratoxin a production in *Aspergillus niger* CBS 513.88 using different carbon sources. Toxins (Basel). 14(8):551. doi: 10.3390/toxins14080551.

Zhan XL, Hong Y, Zhu T, Mitchell AP, Deschenes RJ, Guan KL, Silver P. 2000. Essential functions of protein tyrosine phosphatases PTP2 and PTP3 and RIM11 tyrosine phosphorylation in *Saccharomyces cerevisiae* meiosis and sporulation. Mol Biol Cell. 11(2):663–676. doi: 10.1091/mbc.11.2.663.

Zhao X, Yang X, Lu Z, Wang H, He Z, Zhou G, Luo Z, Zhang Y. 2019. MADS-box transcription factor Mcm1 controls cell cycle, fungal development, cell integrity and virulence in the filamentous insect pathogenic fungus *Beauveria bassiana*. Environ Microbiol. 21(9):3392–3416. doi: 10.1111/1462-2920.14629.